Journal of Molecular Graphics and Modelling 52 (2014) 114–123

Contents lists available at ScienceDirect

Journal of Molecular Graphics and Modelling

journal homepage: www.elsevier.com/locate/JMGM

Protein tyrosine phosphatases: Ligand interaction analysis and optimisation of virtual screening

Mohammad A. Ghattas[a], Noor Atatreh[a], Elena V. Bichenkova[b], Richard A. Bryce[b,*]

[a] College of Pharmacy, Al Ain University of Science and Technology, Al Ain 64141, United Arab Emirates
[b] Manchester Pharmacy School, University of Manchester, Oxford Road, Manchester M13 9PT, UK

ARTICLE INFO

Article history:
Accepted 26 June 2014
Available online 5 July 2014

Keywords:
Protein tyrosine phosphatase
PTP1B
Virtual screening
Docking
Pharmacophore
Constraint

ABSTRACT

Docking-based virtual screening is an established component of structure-based drug discovery. Nevertheless, scoring and ranking of computationally docked ligand libraries still suffer from many false positives. Identifying optimal docking parameters for a target protein prior to virtual screening can improve experimental hit rates. Here, we examine protocols for virtual screening against the important but challenging class of drug target, protein tyrosine phosphatases. In this study, common interaction features were identified from analysis of protein–ligand binding geometries of more than 50 complexed phosphatase crystal structures. It was found that two interactions were consistently formed across all phosphatase inhibitors: (1) a polar contact with the conserved arginine residue, and (2) at least one interaction with the P-loop backbone amide. In order to investigate the significance of these features on phosphatase-ligand binding, a series of seeded virtual screening experiments were conducted on three phosphatase enzymes, PTP1B, Cdc25b and IF2. It was observed that when the conserved arginine and P-loop amide interactions were used as pharmacophoric constraints during docking, enrichment of the virtual screen significantly increased in the three studied phosphatases, by up to a factor of two in some cases. Additionally, the use of such pharmacophoric constraints considerably improved the ability of docking to predict the inhibitor's bound pose, decreasing RMSD to the crystallographic geometry by 43% on average. Constrained docking improved enrichment of screens against both open and closed conformations of PTP1B. Incorporation of an ordered water molecule in PTP1B screening was also found to generally improve enrichment. The knowledge-based computational strategies explored here can potentially inform structure-based design of new phosphatase inhibitors using docking-based virtual screening.

Within the drug discovery process, computational design approaches are now integral [1,2]. An important computational medicinal chemistry tool is molecular docking, which seeks to predict the structure of a complex of two or more molecules. Protein–ligand docking is widely used in the drug discovery area, both in the hit identification and lead optimisation stages [3]. Generally, docking comprises two critical components: the search technique and the scoring function [4]. Although conformational search techniques are reasonably efficient, particularly when applied to small drug-like molecules, scoring functions still required further development [5]. This can pose a problem for virtual screening (VS) of a large library of compounds, where inaccurate scoring of the docked ligand library yields a large number of false positives. The subsequent investigation of these false positives experimentally wastes valuable resources.

Therefore, efforts have been made to optimise the docking approach prior to VS in the hope of limiting virtual false positives and improving experimental hit rates. Approaches to improve docking performance have included evaluating different scoring functions and their effect on ranking docked ligand libraries [6,7]. An alternative approach is to focus on identifying important structural features of ligand and protein, for example, key interactions, presence of water molecules, amino acid rotamers and protein flexibility [8]. As an example of the latter approach, Perola conducted a structural analysis of a large group of kinase enzymes [9] revealing key interactions formed between kinase inhibitors and the backbone amides of the hinge region. Following a series of

Abbreviations: VS, virtual screening; PTP, protein tyrosine phosphatase; PTP1B, protein tyrosine phosphatase-1B; IF2, isoform 2 of low molecular weight protein tyrosine phosphatase; PLIF, protein–ligand interaction fingerprint; EF, enrichment factor; RMSD, root mean square deviation.

* Corresponding author. Tel.: +44 0161 275 8345; fax: +44 0161 275 8360.
E-mail addresses: richard.bryce@manchester.ac.uk, R.A.Bryce@manchester.ac.uk (R.A. Bryce).

http://dx.doi.org/10.1016/j.jmgm.2014.06.011
1093-3263/

docking experiments, it was found that constraining these interactions during docking led to retrieval of a significantly larger number of known kinase inhibitors in the top-ranked docked dataset in comparison to unconstrained docking.

In this study, we investigate the interactions of protein tyrosine phosphatases (PTPs) with their co-crystallized ligands in order to identify features that could enhance their virtual screening. PTPs are a group of enzyme that hydrolyse phosphate from a tyrosine residue [10]. All cysteine-based PTPs share the same signature motif, Cys(XXXXX)Arg, in their catalytic site. Cysteine-based PTPs are generally grouped into three classes according to the amino acid sequence of their catalytic domains [10]. Class I PTPs share a characteristic motif of 250 residues, including the conserved active site motif. PTP1B, a prototypical class I phosphatase, is considered a novel target for type II diabetes mellitus and diet-induced obesity [11]. Class II PTPs are known as low molecular weight PTPs due to their small size, of around 20 kDa. Human low molecular weight PTPs, for example isoform 2 (IF2), are also involved in the pathogenesis of type II diabetes mellitus [12]. Class III phosphatases include only Cdc25 phosphatases which are involved in cell-cycle progression. Cdc25 are cysteine-based PTPs which show catalytic activity against both phosphotyrosine- and phosphoserine/threonine-containing substrates [13]. PTPs are also considered as interesting targets for cancer since both PTP1B and Cdc25 are known to be overexpressed in breast tumour [14] and human low molecular PTPs such as IF2 are known to play a role in tumour onset and growth [15].

In recent years, virtual screening has been applied to the discovery of new PTP inhibitors [16–19]. These computational studies have adopted a conventional preparation of the protein structures for docking, such that all solvent molecules were deleted and no geometric constraints were applied, although there was investigation of scoring function selection. Here, we seek to enhance these approaches by investigating whether there are any amino acid residues common to the PTP family that consistently interact with PTP inhibitors; and then assessing how important these interactions are for improving ligand docking and library ranking. To achieve this, we select a representative of each PTP class, i.e. PTP1B, IF2 and Cdc25b, for structural investigation and subsequent docking experiments.

1. Methods

1.1. Analysis of PTP–ligand complexes

We obtained 51 PTP1B-ligand complexes (listed in *Supporting Information*) and another four complexes, of Cdc25b (PDB: 1QB0, 1CWT and 1CWS [20]) and IF2 (PDB: 1XWW [21]) from the Protein Data Bank [22]. All 55 crystal structures were graphically analysed via the PyMOL program [23] in order to assess ligand–protein interactions. Automated protein–ligand analysis was carried out for the PTP1B–ligand complexes. This was achieved by categorising these crystal structures into two clusters. The first cluster, named 'open', included 7 PTP1B structures whose WPD loop is in the open conformation. The second cluster, named 'closed', included 44 structures whose WPD loop is in the closed conformation. The WPD loop takes the open conformation when PTP1B is in the apo form and, upon substrate binding, it closes downwards to take its part in the catalytic mechanism [24].

For each complex, a protein–ligand interaction fingerprint (PLIF) was generated using the MOE software package [25]. For the PLIF, protein–ligand hydrogen bonds were scored based on heavy atom type, interatomic distance and orientation, derived using a statistical approach trained using a set of experimental protein structures [26]. This score is then expressed as a percentage probability of being a good hydrogen bond. Ionic interactions were scored by calculating the inverse square of the distance between atoms with opposite formal charge (e.g. a carboxylate oxygen atom and a protonated amine), and expressing this as a percentage (such that 100% corresponds to a separation of 1 Å) [25]. Minimum score thresholds for hydrogen bonding and ionic interactions were taken as the default settings of 1% and 5% respectively. Interactions between the active site residues and the co-crystallised ligand atoms that were not able to achieve a higher value than the minimum scores were not considered in the PLIF. The PLIF graph generated then displays the interaction occupancy of all residues in the PTP1B active site. This occupancy is defined as the percentage of ligands interacting with the side chain or main chain of a given amino acid.

1.2. Preparation of test sets

Three test sets were prepared for use in seeded virtual screening against the three PTP enzymes, PTP1B, IF2 and Cdc25b. Each test set consists of two main components: firstly, known PTP inhibitors (PTP1B: 67 ligands; Cdc25b: 38 ligands; IF2: 25 ligands) which were obtained from literature and had a molecular weight of not more than 500 Da (listed in *Supporting Information*). The known inhibitors were considered as active ligands only if they had IC_{50} or K_i values of 50 μM or less. These compounds were either extracted from their original crystal structures or, alternatively, created using MarvinSketch [27]. Secondly, decoy ligands were selected from a commercial database (TimTec [28]) in order to represent inactive ligands. The process of choosing these compounds began by randomly selecting 50,000 ligands with molecular weights of less than 500 Da, each of which was assigned a fingerprint using MACCS structural keys [29]. This algorithm gives a fingerprint based on how many predefined substructures (one to ten non-hydrogen atoms) exist in each ligand. Ligands were then clustered using the Tanimoto coefficient in MOE (thresholds of similarity and overlap of 50%) [25]. Five thousand ligands were taken from 5000 different clusters and then processed via the *wash* module in MOE [25] in order to assign their ionisation state at pH 7. All ligands were assigned partial charges using the MMFF94x force field and energy minimised [30–36].

1.3. Preparation of protein structures for seeded VS experiments

The protein structures, all of resolution <2 Å, were obtained from the PDB: for PTP1B-closed (PDB: 1C88 [37]), for PTP1B-open (PDB: 1G7F [38]), IF2 (PDB: 1XWW [21]) and Cdc25b (PDB: 1QB0 [20]). Using the MOE *3D protonate* module [25], hydrogen atoms were added to each enzyme and partial charges were assigned on each atom based on the MMFF94 force field [31–35]. All water molecules were removed from the PTP1B open, IF2 and Cdc25b structures prior protein preparation. For the PTP1B closed conformation, two structures were prepared: the first was constructed without water; and the second with all water removed, apart from the ordered water molecule that was observed to be buried behind the WPD loop.

1.4. Docking protocols

Prior to docking, an Arg/P-loop pharmacophore was designed using the MOE Pharmacophore Elucidation module for use in the constrained docking protocol [25]. Two pharmacophore points were set up based on the coordinates of the two terminal oxygen atoms bound to the conserved Arg side chain and/or the P-loop backbone amide. Both pharmacophore points accept an anionic group (An) and/or a hydrogen bond acceptor (HBA). Consequently, co-crystallised ligands of the three PTP enzymes used in the seeding experiments were employed to define the protein catalytic site.

Then, the three test sets were docked into their corresponding protein active site using the MOE-Dock program, where Triangle Match and Pharmacophore were employed as placement methods in the free (denoted *Dock*) and constrained (*Dock/PH4*) docking protocols, respectively. In former algorithm, two sets of triplet atoms are created for both the ligand and the active site; these are then matched together to produce multiple docking solutions. In the Pharmacophore algorithm, the ligand is placed using the features in the previously defined pharmacophore and then oriented to obtain the best fit. The London ΔG scoring function [25] was used for ranking poses generated from both docking protocols; only the top scoring pose was considered in the final docking output. The London ΔG score is calculated as follows:

$$\Delta G = c + E_{\text{flex}} + \sum_{\text{hbonds}} c_{\text{HB}} f_{\text{HB}} + \sum_{\text{m-lig}} c_{\text{M}} f_{\text{M}} + \sum_{i} \Delta D_i \quad (1)$$

where c accounts for the average change in rotational and translational entropy; E_{flex} is the energy due to the loss of flexibility of the ligand; f_{HB} quantifies geometric deviation in hydrogen bonds; c_{HB} is the energy of an ideal hydrogen bond; f_{M} measures geometric deviation in metal ligation; c_{M} is the energy of an ideal metal ligation; and ΔD_i is difference in desolvation energy of atom i on binding. In the constrained docking protocol, binding constraints to the two previously defined pharmacophoric points were employed. Only poses that met at least one of the two pharmacophoric features were considered for scoring. Known inhibitors featuring in the top 1%, 3%, 5% and 10% of the ranked library of compounds were counted in order to calculate the enrichment factor (EF). EF for the top n% of the ranked library was defined as follows:

$$EF_{n\%} = \frac{a}{A} \times 100\% \quad (2)$$

where a is the number of inhibitors in the top n% of the ranked library, and A is the total number of known inhibitors.

1.5. Robustness of docking analysis

An analysis of docking robustness was conducted on the PTP1B enzyme. A total of 26 PTP1B structures were obtained from the Protein Data Bank [22] and then aligned on the protein structure with PDB code 1C88 (the reference X-ray structure used in the PTP1B seeded VS experiments). All protein structures were prepared for docking using the MOE *3D protonate* module [25] in order to add hydrogens and assign partial charges. The co-crystallised ligands were extracted from their original crystal structures. Subsequently, ionisation states of titratable groups were assigned using the *wash* module in MOE and each co-crystallised ligand was then saved separately. Following the washing process, MOE was used to assign partial charges for each ligand and then to energy minimise them using the MMFF94x force field [30–36].

As before, docking was performed using MOE-Dock [25] via Triangle Match and Pharmacophore placement methods in the unconstrained and constrained docking protocols respectively, in conjunction with the London ΔG scoring function. The two-point pharmacophore was included in all constrained docking experiments. The known ordered water molecule was included in docking where applicable. The heavy-atom RMSD in distance of the top-ranked pose of each co-crystallised ligand was measured with respect to its bound X-ray conformation [39].

2. Results and discussion

2.1. Analysis of ligand–PTP complexes

First, we analyse the target active site to better understanding the key interactions necessary for ligand binding to PTPs [40]. To this end, a set of more than 50 PTP–ligand complexes were considered, involving the three enzymes, PTP1B, IF2 and Cdc25b, one from each of the three main PTP classes, I-III. PTP1B is the most widely studied of these enzymes and thus had the largest number of crystal structures of the PTPs in the Protein Data Bank. PTP1B is known to have a flexible loop, the WPD loop, that can adopt two different conformations upon ligand binding, closed or open (Fig. 1). The closed conformation is more common amongst PTP1B crystal structures [41], featuring in 44 out of the 51 structures used here. Also, an ordered water molecule that is buried just behind the WPD loop in the closed configuration has been observed in a number of PTP1B crystal structures (Fig. 1) [37,42–46]. These features seem to be specific to PTP1B and have not been observed in IF2 or Cdc25b.

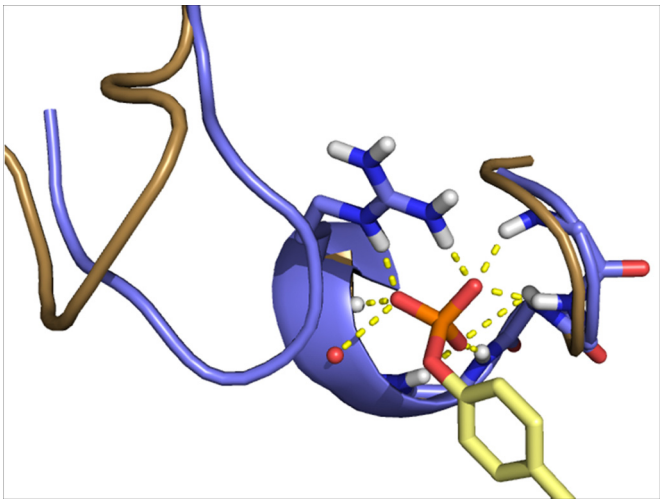

Fig. 1. Structural alignment of apo PTP1B in open conformation (1G7F [38], gold) with PTP1B in closed conformation (1G1G [43], blue). The latter appears with its buried water (red sphere) and its co-crystallized ligand (yellow).

All PTP enzymes have a conserved $C(X)_5R$ motif in the P-loop of their catalytic sites; these amino acids have important roles in the PTP catalytic mechanism [47]. The cysteine residue is proposed to be involved in nucleophilic attack at the substrate phosphorus atom. The P-loop backbone amide and side chain of the conserved arginine residue has been implicated in substrate recognition, as well as in stabilisation of the transition state and enzyme-product complex, via binding to the phosphate oxygen atoms of the substrate. The side chain of this Arg also appears to serve in keeping the WPD-loop proximal to the site of catalysis: the Arg hydrogen bonds with the Trp backbone amide of the WPD-loop, facilitating activation of the hydrolytic water molecule by the Asp of the loop [47]. Therefore, it was important to evaluate if these conserved amino acids are similarly important in binding to PTP inhibitors. To investigate this, the experimental geometries of 55 protein–ligand complexes, comprising 51 PTP1B structures, three Cdc25b structures and one IF2 structure were visually inspected. This analysis showed that all of the crystal structures of the three PTP enzymes have their co-crystallized ligands consistently bound to the conserved Arg side chain and P-loop backbone amides (for example, as in Fig. 1 for the closed form of PTP1B).

As PTP1B has a large number of crystal structures in the PDB compared to IF2 and Cdc25b, automated analysis was also conducted on the PTP1B–ligand complexes: protein–ligand interaction fingerprints (PLIF) were generated for each PTP1B-inhibitor complex, namely the 44 'closed' and 7 'open' structures (Fig. 2). The side chain and backbone amide interactions of each active site residue in PTP1B was scored. 19 residues were found to contribute to the stabilisation of ligands in the 'closed' PTP1B structures (Fig. 2A); (for clarity, we note that only the amino acids involved in the

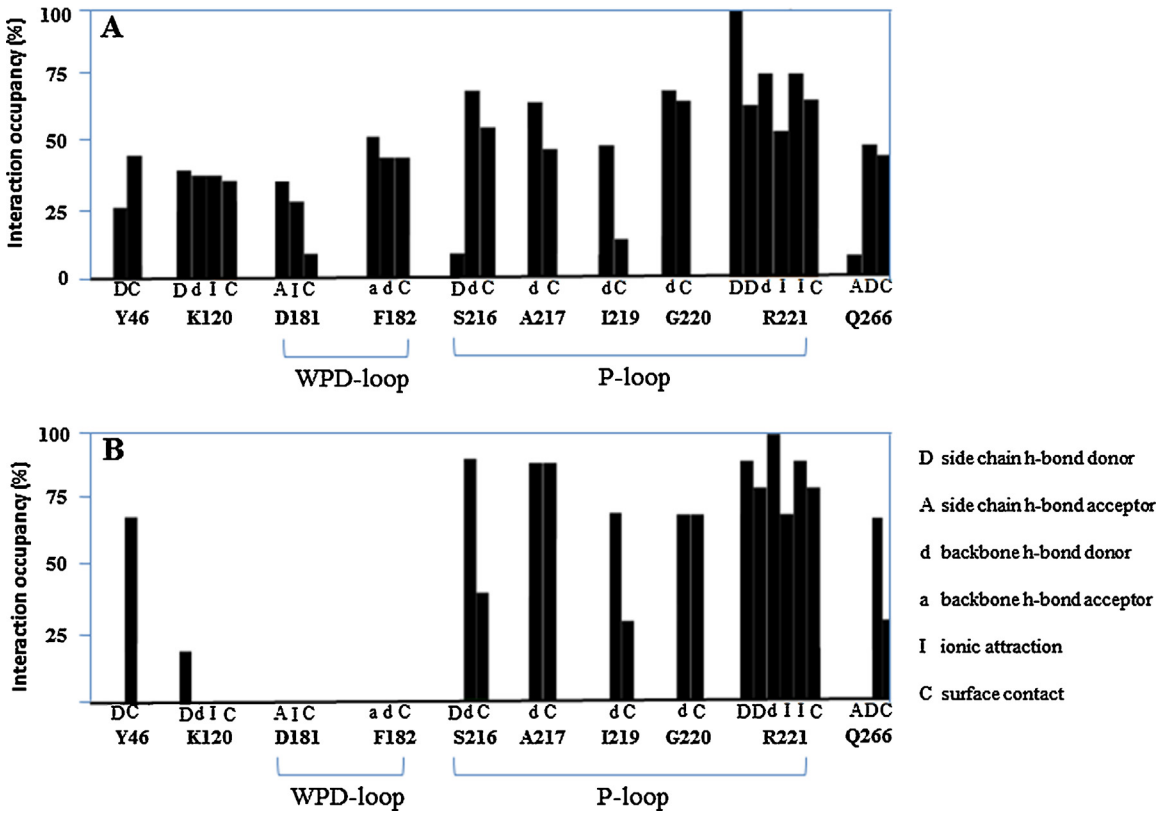

Fig. 2. (A) PLIFs of 44 ligand–protein complexes in closed WPD loop conformation of PTP1B; (B) PLIFs of seven ligand–protein complexes in open WPD loop conformation of PTP1B. For clarity, only amino acids involved in the greatest number of interactions are shown.

greatest number of interactions are shown in Fig. 2). 15 residues were involved in the ligand–protein interactions for the 'open' PTP1B structures (Fig. 2B). The difference in number of contributing residues between closed and open is largely due to the displacement that takes place on opening of the WPD loop conformation, which removes the WPD loop residues from contact with the bound ligand.

In the closed PTP1B conformation, the PLIF profile emphasises the importance of the conserved arginine, Arg221, for stabilising inhibitors in the catalytic pocket: all tested complexes appear to involve at least one hydrogen bond with the Arg221 side chain, with an occupancy of 100% (Fig. 2A). By contrast, in the open conformation, the backbone amide of Arg221 seems to be slightly more critical than the side chain for stabilising the known PTP1B inhibitors, with interaction occupancies of 100% and 90% respectively (Fig. 2B). The P-loop backbone amides of Ser216 and Ala217 are also capable of making ligand interactions, with occupancies of 60–90% respectively, with equal measure in open and closed PTP1B conformations (Fig. 2A and B). Therefore, one electrostatic interaction with the conserved Arg residue and at least one hydrogen bond with a P-loop backbone amide appears to be crucial for ligand binding in the PTP1B pocket. Inspection of the IF2 and Cdc25b crystal structures finds that these protein–ligand interactions are also made. Thus all 55 PTP inhibitors interact with the Arg and P-loop in this way. From inspection of the PTP1B, Cdc25b and IF2 crystal complexes, all co-crystallized ligands appear to have a polar head on their structures, with one or two hydrogen bond acceptors that are buried deeply in the active site and make the crucial electrostatic interactions observed in our PLIF study (for example, PTP1B in Fig. 1). The similarity of ligand binding interactions for the PTP1B, Cdc25b and IF2 crystal structures suggests that their specific features could be used as constraints to enhance screens targetting the PTP active site.

2.2. Seeded virtual screening experiments

The above structural study of three PTP enzymes highlights interactions likely to be essential for good ligand binding in the PTP catalytic site. We also note that the presence of a buried water molecule in many PTP1B-ligand crystal structures could play a role in PTP1B inhibitor binding. The effect of these factors on virtual screening can be assessed by performing a series of seeding experiments against different PTP enzymes. Seeding involves mixing experimentally known inhibitors of the target with presumed inactive ligands which are then docked into the target active site twice, in this case in the presence and absence of constraints. Subsequently, enrichment factors for the two screens are compared, calculated based on Eq. (2) [40].

2.3. Test sets for seeded virtual screening experiments

Three test sets were prepared for use in the seeded VS experiments of PTP1B, IF2 and Cdc25b. Each test set comprised two parts, one containing the known inhibitors and another the decoy ligands. In order to avoid bias in the structures of the decoy ligands, they were selected from a large collection of clustered compounds (see Section 1.2). Active ligands for each of the three target enzymes were added to this structurally diverse decoy ligand set to form three separate test sets.

We first consider the physicochemical property profiles for the decoy and three active ligand groups (Table 1). The calculated properties of active ligands and decoy ligands have a mean value lying within the range of drug-like properties, as defined by Lipinski and Veber [48,49]. The known inhibitors of IF2, in particular, had a greater molecular weight and log P on average than the decoy ligands, a function of their large size (Table 1). However, these inhibitors were amongst the very few compounds found in the

Table 1
Mean values of the physicochemical properties of the test sets used in the PTP seeding experiments, for #RB number of rotatable bonds (RB); molecular weight (M.Wt); log *P* = number of hydrogen bond donors (HBD); number of hydrogen bond acceptors (HBA); and topological polar surface area (TPSA). Range in parentheses.

Physico-chemical properties	Dug-like range	Decoy ligands included in the three test sets	Active ligands of each test set		
			PTP1B	Cdc25b	IF2
$N_{compounds}$	–	5000	67	38	25
RB	≤10	4.67 (0–25)	5.82 (1–15)	3.30 (0–11)	4.14 (0–6)
M.Wt (Da)	≤500	303.9 (84–500)	376.8 (194–497)	343.8 (194–493)	409.7 (278–493)
log *P*	≤5	3.13 (−6.5 to 10.6)	4.13 (−0.8 to 9.9)	3.51 (2.0–6.2)	4.92 (−0.3 to 7.4)
HBD	≤5	1.28 (0–10)	0.99 (0–5)	1.08 (0–4)	2.52 (1–5)
HBA	≤10	4.29 (0–14)	5.52 (1–12)	5.30 (1–10)	5.12 (3–8)
TPSA (Å^2)	≤140	63.5 (0–219)	85.5 (9–183)	77.7 (20–123)	91.5 (49–133)

literature to inhibit IF2. We also note that the mean topological polar surface area (TPSA) was found to differ slightly between the decoy ligand and known inhibitor sets. Whereas the decoy ligands have a TPSA mean value of 64 Å^2, the active ligands have greater mean values, ranging from 78 to 92 Å^2. Nevertheless, whilst the means differ to a degree, the TPSA range for the decoy set comfortably encompasses that of the three active ligand sets.

2.3.1. *Effect of adding constraint on Arg/P-loop*

In order to evaluate the influence of ligand interactions with the conserved Arg and P-loop backbone amides on the PTP virtual screens, two docking protocols were conducted on each enzyme using the MOE-Dock program [50]: (1) an unconstrained docking protocol, which we denote *Dock*, and (2) a constrained docking protocol, denoted *Dock/PH4*. In the free docking protocol, the Triangle Matcher (TM) method [25] was used for sampling of bound poses. In the constrained docking protocol, the Pharmacophore (PH4) method [25] was used in the placement stage, where a pre-defined two-point pharmacophore was used to guide the placement of the ligand atoms. This pharmacophore was created based on the co-crystallized ligand polar head: it contained two HBA/Anion points located within a heavy atom interaction distance of less than 4 Å from the conserved Arg side chain and the P-loop backbone amides (Fig. 3). The Pharmacophore method generated poses that satisfies at least one of the two pre-defined pharmacophoric features. This means that all poses generated by this method were directed to make at least one of the required key interactions with the PTP. Scoring and ranking of docked poses in both protocols was performed using the London ΔG scoring function, and then EFs were calculated for each docking protocol.

Enrichment factors were obtained from virtual screening using the two docking protocols on the three PTP systems (Table 2). Firstly, for screening with the *Dock* protocol, we find that the $EF_{5\%}$ values of the IF2 and Cdc25b screens are similar ($EF_{5\%}$ of 16). For PTP1B, the enrichment is found to be even higher, for both closed and open conformations; here, the $EF_{5\%}$ values range between 40 and 48 respectively (Table 2). In comparison with the *Dock* screen, screening with the constrained *Dock/PH4* docking protocol increases the $EF_{5\%}$ values by up to a factor of 2 (Fig. 4, Table 2). Similarly, the enrichment improved for the IF2 screen when the Arg/P-loop pharmacophoric constraint was applied, from 16 to 32 (Table 2). For Cdc25b, a dual specificity PTP, the EF increased by 67% when constrained docking was used. Whilst the EFs of PTP1B obtained from the free virtual screens were already quite high compared to the Cdc25b and IF2 enrichments, applying the *Dock/PH4* protocol led to further enrichment. Indeed, the constrained docking screen was able to enhance the number of retrieved inhibitors in the top 5% portion by 33% and 25% in the closed and open PTP1B conformations, respectively. Thus, constrained docking had a positive influence on the screens against all three PTPs and could potentially have a similar benefit on screens against other PTP enzymes.

Dock/PH4 constrained VS improved enrichment over *Dock* for both the open as well as closed conformation of PTP1B (Table 2). Interestingly, the more spacious binding pocket of the PTP open, inactive conformation has been specifically and successfully targeted recently via VS, leading to several compounds with potent inhibition activity (e.g. the PTPσ and PTPN22 enzymes); these inhibitors are thought to stabilise the open WPD-loop conformation and in this way prevent catalysis of dephosphorylation [24,51].

The set of decoys used in the screens above are a diverse set of compounds typical of a commercially available ligand library. However, as noted in Section 2.3, the set of 5000 decoys have a mean TPSA value of 64 Å^2, which is slightly lower than the mean values for the known inhibitor sets (78–92 Å^2, Table 1). Additionally, the actives are on average slightly larger than the decoys, by 70 Da

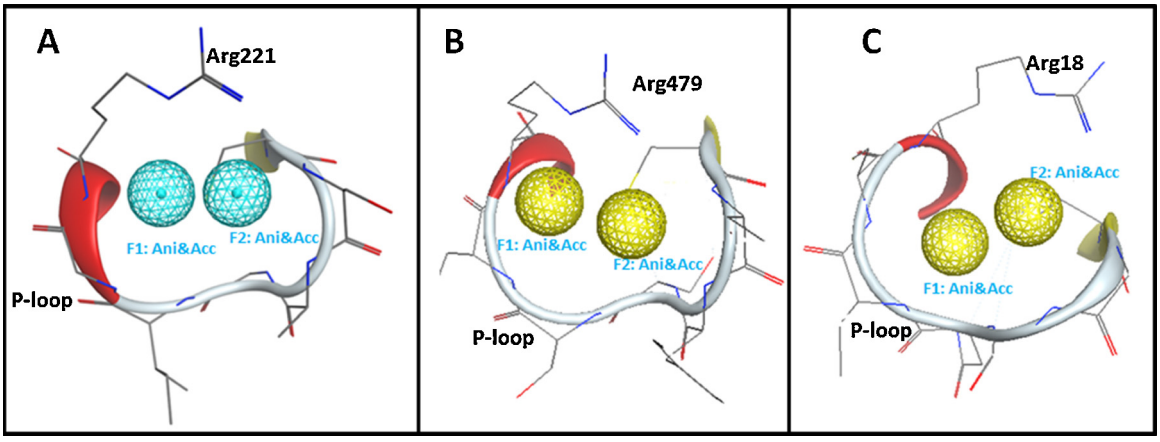

Fig. 3. Pharmacophore for (A) PTP1B (blue), (B) Cdc25b (gold) and (C) IF2 (gold). Some of the protein structure is not shown for clarity.

Table 2
Enrichment factors from free docking and constrained docking protocols in three PTP enzymes at different top ranked library percentages.

Top ranked library %	PTP1B (closed)		PTP1B (open)		Cdc25b		IF2	
	Dock	*Dock/PH4*	*Dock*	*Dock/PH4*	*Dock*	*Dock/PH4*	*Dock*	*Dock/PH4*
Top 1%	13.4	22.4	19.4	20.9	0.0	0.0	0.0	0.0
Top 3%	34.3	41.8	35.8	44.6	7.9	15.8	12.0	16.0
Top 5%	40.3	53.7	47.8	59.7	15.8	26.3	16.0	32.0
Top 10%	53.7	62.7	62.7	65.7	26.3	31.6	20.0	44.0

Table 3
Enrichment factors (EF) obtained from free (*Dock*) and constrained (*Dock/PH4*) docking of the large polar compound subset in the closed and open PTP1B.

Top ranked library %	PTP1B–EF			
	Closed conformation		Open conformation	
	Dock	*Dock/PH4*	*Dock*	*Dock/PH4*
Top 1%	6.0	14.9	10.5	11.9
Top 3%	25.4	32.8	26.9	28.4
Top 5%	35.8	41.8	31.3	38.8
Top 10%	46.3	59.7	52.2	59.7

Table 4
The RMSD average values of the 26 ligands docked into their co-crystallized PTP1B structure.

Enzyme	Average RMSD (Å)			
	Dock	*Dock/Wat*	*Dock/PH4*	*Dock/PH4/Wat*
PTP1B/closed	4.11	3.22	2.34	2.30

(Table 1). In order to assess the effect of this on the screen, a subset of 1730 decoys were selected from the 5000, with average molecular weight and TPSA values of 372.6 Da and 81 Å^2, respectively. These properties compare closely to the corresponding average molecular weight and TPSA of the set of known PTP1B inhibitors, with values of 376.8 Da and 85.5 Å^2, respectively. Then, the new test set of PTP1B actives and 1730 decoys was docked into the PTP1B open and closed conformation of PTP1B using the *Dock* and *Dock/PH4* docking protocols. Gratifyingly, for this larger and more polar decoy subset, it is clear that the *Dock/PH4* approach improves over *Dock*. Thus the *Dock* method has $EF_{5\%}$ values of 36 and 31 for closed and open PTP1B conformations respectively (Table 3) – these enrichments are reduced from $EF_{5\%}$ values of 40 and 48 when using the full 5000 decoys set (Table 2). Including the constraint on the screening in the *Dock/PH4* approach improves over *Dock* by 17% and 26% to $EF_{5\%}$ values of 42 and 39 for closed and open conformations respectively (Table 3).

Previous studies on virtual screening have highlighted the importance of accurate prediction of binding mode in order to properly score and rank active compounds and thus discriminate them successfully from inactive ligands in a compound library [9,52]. It is also important to ensure that an improvement in enrichment is not associated with a worsening in prediction of bound pose; potentially a constraint-directed docking could distort well docked poses in order to satisfy the predefined pharmacophore. Therefore, a series of validation experiments to assess the robustness of docking were carried out, in which the RMSD distance was measured for a docked ligand pose with respect to its crystallographic bound conformation [53,54]. Accordingly, out of a set of 67 PTP ligands, 26 had X-ray structures co-crystalized PTP1B inhibitors that were included in the PTP1B virtual screens. Each of these 26 compounds was investigated separately by docking them into its own co-crystallized protein active site, using the two docking protocols.

We find that the *Dock/PH4* approach, with the Arg/P-loop constraint, was able to improve the mean RMSD in distance to the X-ray bound conformation by 43%, decreasing from 4.1 to 2.3 Å (Table 4). Almost half the docked ligands (12 out of 26) exhibited a significant improvement in their predicted bound conformation, with an RMSD improvement of >1 Å, when the constrained docking protocol was applied (Fig. 5). The most noticeable improvement was shown by 1XBO, an isoxazole carboxylic acid inhibitor [55]. Compared to its X-ray conformation (Fig. 6A), the RMSD value decreased from 10.2 to 2.4 Å when constrained docking was employed. It seems the free protocol docked the 1XBO ligand in the opposite

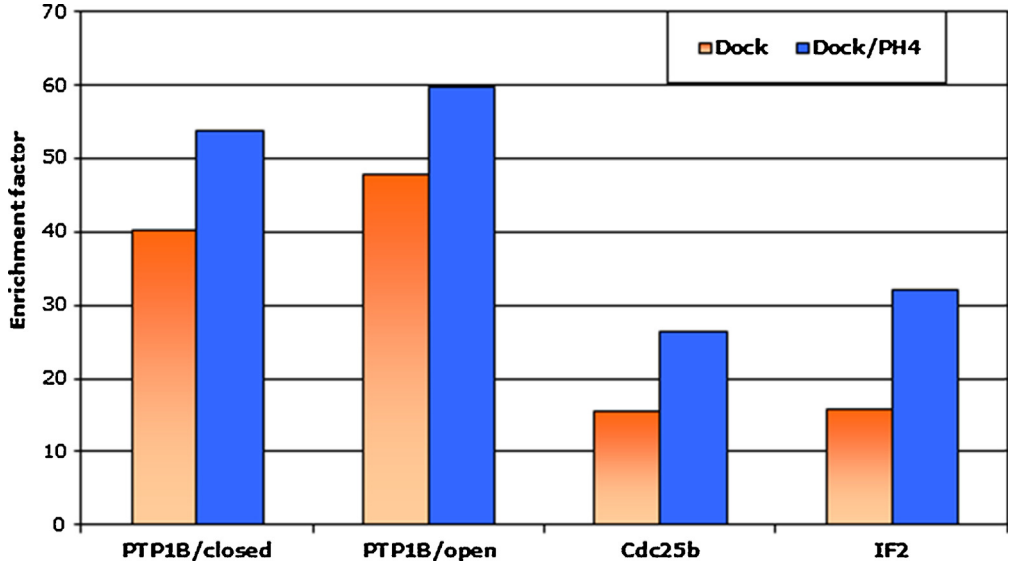

Fig. 4. Enrichment factors at the top 5% for virtual screening against PTP1B (closed and open), Cdc25b and IF2, using the free (*Dock*) and constrained docking (*Dock/PH4*) protocols.

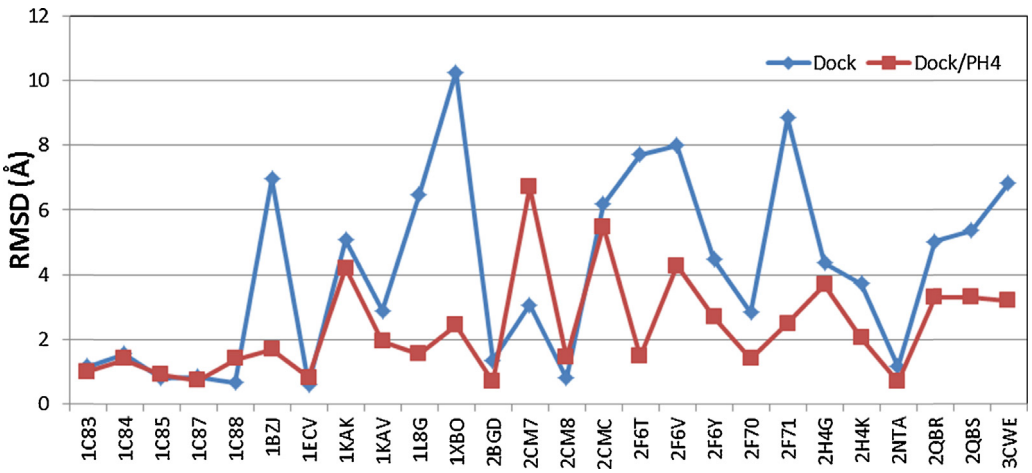

Fig. 5. Heavy atom RMSD distance values (in Å) of 26 co-crystallized PTP1B inhibitor poses, docked using *Dock* and *Dock/PH4* protocols, with respect to their X-ray geometries.

orientation (Fig. 6B); constrained docking was more successful in reproducing the X-ray conformation by requiring the docking algorithm to place the ligand polar head in the correct position, in order to satisfy the pre-defined pharmacophore (Fig. 6C). Therefore, the pharmacophore-directed docking ensured the ligand carboxylate made the key electrostatic interactions with the Arg side chain and P-loop backbone amides.

Interestingly, one ligand out of the 26 docked inhibitors, 2CM7 [56], had its X-ray conformation more accurately predicted by *Dock* relative to *Dock/PH4*, with an RMSD increase from 3.0 to 6.7 Å respectively (Fig. 5). However, only the tail of 2CM7 seemed to be placed incorrectly by constrained docking (Fig. 7C) compared to free docking (Fig. 7B), as the polar head was positioned correctly by both protocols, according to the X-ray conformation (Fig. 7A). Thus, the Arg/P-loop constraint seems to play no role in the 2CM7 tail misprediction, since the polar head was able to make the key interaction with or without the use of the pharmacophoric constraint.

Therefore, our seeding and robustness of docking experiments show that inclusion of the Arg221/P-loop constraint in docking/screening was not only able to improve the enrichment of PTP1B inhibitors, but also, in restricting the docking search space, enhanced the overall quality of the predicted poses.

2.4. Effect of water

As noted above, in the closed structure of many crystallographic PTP1B–ligand complexes, an ordered water molecule is located proximal to the P-loop in the PTP1B active site; this water is thought to have a role in stabilising the WPD-loop in the closed conformation (Fig. 1) [43,57]. Furthermore, the water forms hydrogen bonds with almost all ligands that were co-crystallized with PTP1B in its closed conformation. Consequently, it is important to consider its effect on docking and enrichment [8].

The PTP1B test set was docked into the PTP1B active site in the presence and absence of the ordered water using both *Dock* and *Dock/PH4* protocols (Table 5). Inclusion of the ordered water improved enrichment using the *Dock* method. For example, the enrichment increased by 26% using the water-based docking protocol, *Dock/Wat* ($EF_{5\%}$ of 51, Table 5) compared to docking without the water molecule, *Dock* ($EF_{5\%}$ of 40). In the constrained protocol, the effect of the ordered water was less clear: improved enrichment was seen at the 1% and 3% levels, but not at the 5% and 10% levels (Table 5). Nevertheless, overall, at the 1% level, the enrichment obtained from *Dock/PH4/Wat* was double ($EF_{1\%}$ of 27, Table 5) that of *Dock* ($EF_{1\%}$ of 13). This broadly positive influence of the ordered water observed here is consistent with a 3D QSAR study showing

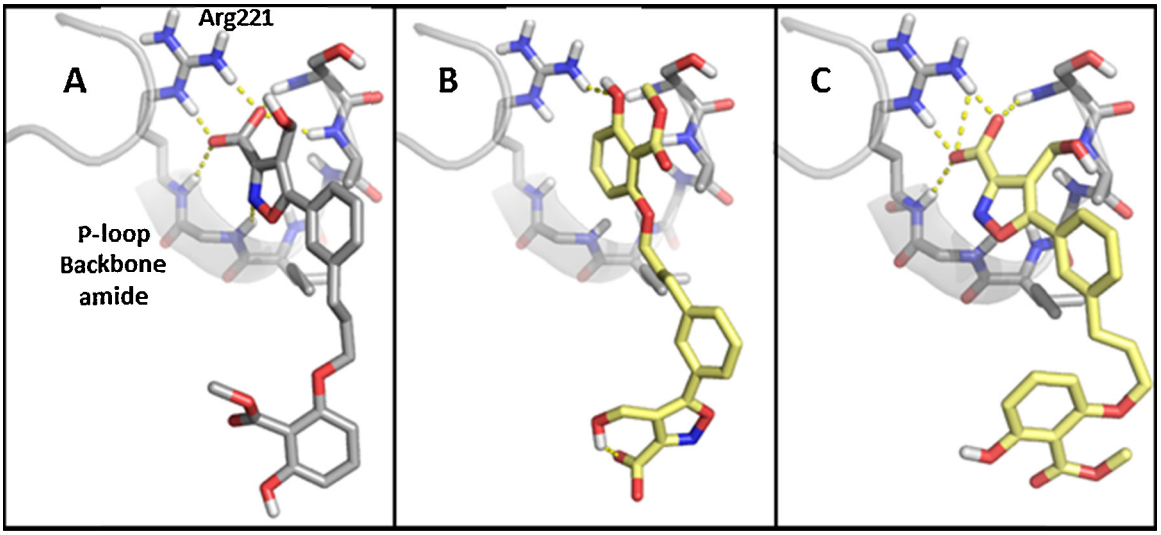

Fig. 6. X-ray conformation of (A) 1XBO [55] (grey) and the docked poses (yellow) from (B) *Dock* and (C) *Dock/PH4* protocols. Some of the protein structure is not shown for clarity.

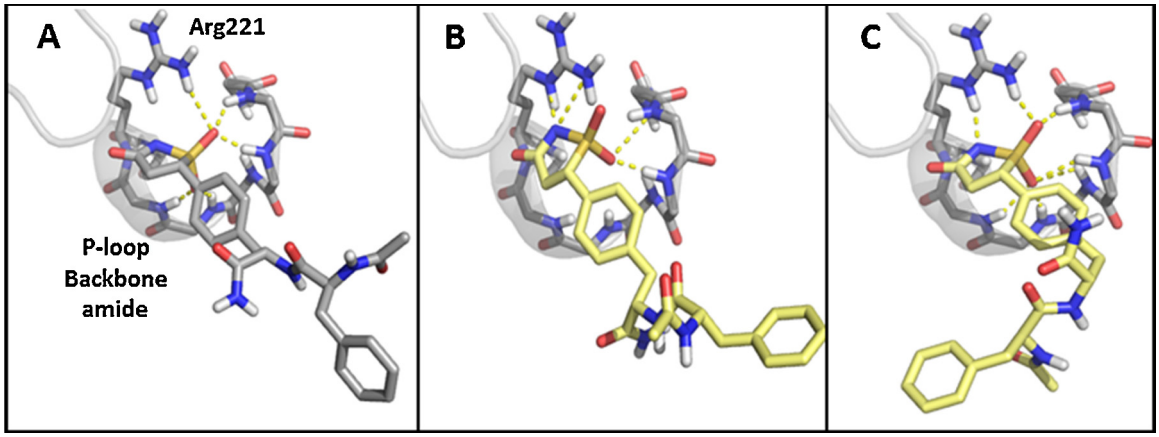

Fig. 7. X-ray conformation of (A) 2CM7 [56] (grey) and docked poses (yellow) from (B) *Dock* and (C) *Dock/PH4* protocols. Some of the protein structure is not shown for clarity.

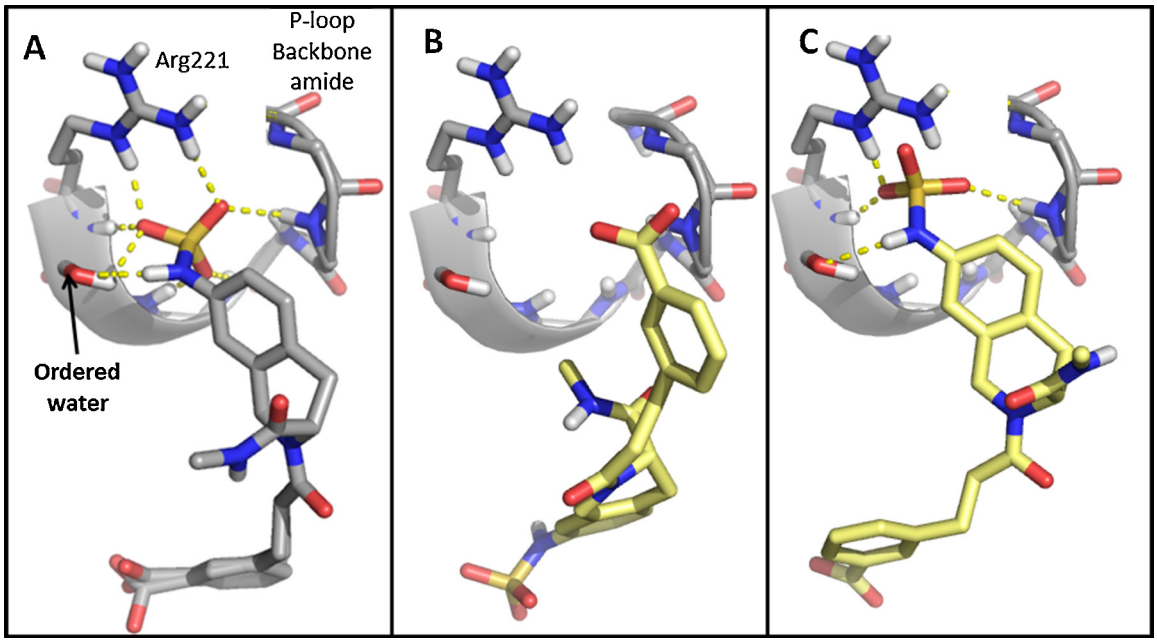

Fig. 8. X-ray conformation of (A) 2F71 [63] (grey) and docked poses (yellow) from (B) *Dock* and (C) *Dock/Wat* docking. Some of the protein structure is not shown for clarity.

that the most predictive model was achieved when the PTP1B active site was hydrated [58]. We recognise, of course, that here we model the effect of one, commonly bound water molecule, rather than all water molecules of hydration found within a given crystal structure of the PTP1B enzyme.

Finally, the effect of the ordered water on docking accuracy was studied. We find that the presence of the ordered water during the unconstrained placement of ligands improved the ability of docking to reproduce the X-ray conformation of the known PTP1B inhibitors, such that the average RMSD value decreased from 4.1 to 3.2 Å (Table 4). Inclusion of the water into the constrained docking protocol did not improve the mean RMSD, both approaches having a value of 2.3 Å (Table 4), suggesting the water and constraint may be having similar effects on docking pose. In improving ligand placement in *Dock*, the water molecule provides valuable additional sites of interaction for ligands. This is clearly shown by the 2F71 ligand which docked incorrectly in the absence of water compared to its X-ray conformation (Fig. 8A), with an RMSD of 8.9 Å (Fig. 8B). The docking gave an improved solution when the ordered water molecule was kept in the active site, such that the RMSD decreased from 8.9 to 2.6 Å (Fig. 8C). Nonetheless, including water during docking should be used with caution in order to not to miss compounds in a PTP1B virtual screen, such as the isothiazolidinone inhibitors which displace this water; this can be achieved for example by using docking software that is able to displace the ordered water molecule when needed, such as the FITTED program [59].

Thus, assessment of docking pose prediction indicates that utilising the Arg/P-loop constraint during docking, with or without the ordered water molecule, ensured the best prediction of the bound conformation of the known inhibitors (Fig. 9A). As discussed above, improved enrichment is observed in all cases for inclusion of the constraints; improvement is also generally seen on inclusion of the

Table 5
Enrichment factors (EF) obtained from four docking protocols in the closed PTP1B enzyme, at different top ranking portions.

Top ranked library %	PTP1B (closed) – EF			
	Dock	*Dock/Wat*	*Dock/PH4*	*Dock/PH4/Wat*
Top 1%	13.4	16.4	22.4	26.9
Top 3%	34.3	44.8	41.8	43.3
Top 5%	40.3	50.7	53.7	46.2
Top 10%	53.7	58.2	62.7	59.7

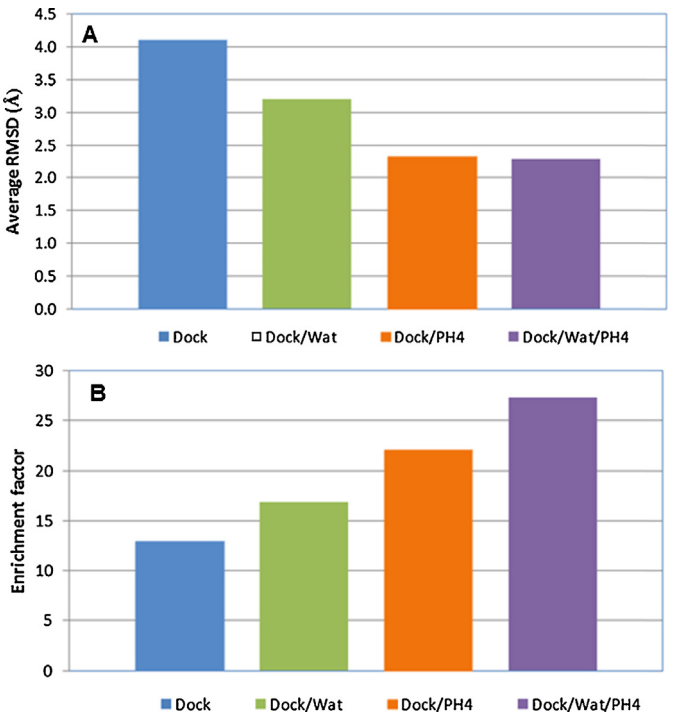

Fig. 9. (A) Mean heavy atom RMSD distance from X-ray geometry (in Å) of the PTP1B-closed inhibitor poses obtained from free (*Dock*) and constrained docking (*Dock/PH4*) protocols, and the same but conducted in the presence (*Dock/PH4/Wat*) and absence of water (*Dock/Wat*); and (B) enrichment factors at the top 1% of PTP1B virtual screen.

Table 6
Average London ΔG scores of true positives (TP) and decoys obtained from top 1% of ranking of PTP1B closed conformation using different docking protocols.

Protein	Score (kcal/mol)			
	Dock	*Dock/Wat*	*Dock/PH4*	*Dock/PH4/Wat*
TP	−15.9	−17.1	−16.4	−17.2
Decoy	−16.1	−16.7	−15.8	−16.6

water molecule. Indeed, a pattern of additivity can be seen in $EF_{1\%}$, when the ordered water molecule and the Arg/P-loop constraint are successively included in the docking procedure of the virtual screen (Fig. 9B). The *Dock/PH4/Wat* method was able to retrieve the greatest number of known PTP1B inhibitors with an $EF_{1\%}$ value of 27 compared to 13 via the *Dock* protocol. These results clearly indicate the importance of the use of these two factors in the PTP1B virtual screens.

This enrichment pattern can be explained by considering the average docking scores of true positives and decoys ranked in the top 1% of the PTP1B closed conformation screens (Table 6). The presence of the ordered water seems to serve as an extra site of interaction, as the average docking scores of the true positives and decoys improved with water by 8% and 4%, respectively. The greater improvement in the docking scores of the true positives may indicate why the *Dock/Wat* screen was able to retrieve a larger number of known inhibitors compared to the *Dock* screen. The improvement of the *Dock/PH4* approach over *Dock* seems to be due to the pharmacophoric constraints' ability to improve the docking scores assigned for known inhibitors, where the average score decreased from −15.9 to −16.4 kcal/mol (Table 6); and, to a lesser extent, to correct the overestimated scores given to decoy ligands, such that the average score for the decoys increased from −16.1 to −15.8 kcal/mol (Table 6). In other words, the Arg/P-loop constraints assisted the docking/scoring algorithm to maximise the number of true binders whilst eliminating some of decoy ligands from the top of the ranking. Previous studies indicated that, as might be expected, the correct prediction of the bound conformation can lead to more accurate ranking [9,52]. That appears to be the case here; the pharmacophoric constraint improved the docking accuracy which causes the known inhibitors to score more favourably and thus improve their ranking in the *Dock/PH4* screens.

3. Conclusions

Analysis of protein–ligand interactions for a set of 55 PTP–ligand complexes revealed that two PTP interaction sites were common to all PTP ligands, namely the conserved Arg residue and the P-loop backbone amides. We observe that incorporation of pharmacophoric constraints on these key interactions in docking was clearly able to influence both the ranking of known PTP inhibitors in virtual screening and the ability to reproduce their experimentally observed bound pose. A similar effect was achieved by the inclusion of an ordered water molecule in the PTP1B virtual screens, where its presence was able to significantly increase the number of true positives in the virtual screen, along with giving improved bound poses. We also note that the PTP1B structure in open and closed WPD-loop conformations demonstrated improvements in enrichment when the interaction constraint was included.

We observe that constrained docking for virtual screening has been employed as an effective tool in improving enrichment for kinases [9], yielding identification of new inhibitors targeting the kinase domain of the fibroblast growth factor receptor 1 [60]. Similarly, pharmacophore constraints in docking-based virtual screening of trihydroxynaphthalene reductase [61] led to identification of an inhibitor with low micromolar activity. Combining ligand-based and target-based approaches, as in our work on PTPs here, appear to be an increasingly attractive approach in performing virtual screens leading to improved experimental hit rates [62].

Acknowledgements

This work was funded by a grant from the Deanship of Scientific Research and Graduate Studies at Al Ain University of Science and Technology, Al Ain, UAE.

Appendix A. Supplementary data

Supplementary material related to this article can be found, in the online version, at http://dx.doi.org/10.1016/j.jmgm.2014.06.011.

References

[1] T.N. Doman, et al., Molecular docking and high-throughput screening for novel inhibitors of protein tyrosine phosphatase-1B, J. Med. Chem. 45 (11) (2002) 2213–2221.
[2] E. Bielska, et al., Virtual screening strategies in drug design – methods and applications, J. Biotechnol. Comput. Biol. Bionanotechnol. 92 (3) (2011) 249–264.
[3] C. McInnes, Virtual screening strategies in drug discovery, Curr. Opin. Chem. Biol. 11 (5) (2007) 494–502.
[4] D.B. Kitchen, et al., Docking and scoring in virtual screening for drug discovery: methods and applications, Nat. Rev. Drug Discov. 3 (11) (2004) 935–949.
[5] D. Plewczynski, et al., Can we trust docking results? Evaluation of seven commonly used programs on PDBbind database, J. Comput. Chem. 32 (4) (2011) 742–755.
[6] P.C.D. Hawkins, A.G. Skillman, A. Nicholls, Comparison of shape-matching and docking as virtual screening tools, J. Med. Chem. 50 (1) (2006) 74–82.
[7] M. Stahl, M. Rarey, Detailed analysis of scoring functions for virtual screening, J. Med. Chem. 44 (7) (2001) 1035–1042.
[8] T. Cheng, et al., Structure-based virtual screening for drug discovery: a problem-centric review, Am. Assoc. Pharmaceut. Scientists J. 14 (1) (2012) 133–141.
[9] E. Perola, Minimizing false positives in kinase virtual screens, Proteins: Struct. Funct. Bioinformat. 64 (2) (2006) 422–435.
[10] H.W. Laurent Bialy, Inhibitors of protein tyrosine phosphatases: next-generation drugs? Angew. Chem. Int. Ed. 44 (25) (2005) 3814–3839.

[11] M. Elchebly, et al., Increased insulin sensitivity and obesity resistance in mice lacking the protein tyrosine phosphatase-1B gene, Science 283 (5407) (1999) 1544–1548.
[12] G. Raugei, G. Ramponi, P. Chiarugi, Low molecular weight protein tyrosine phosphatases: small, but smart, Cell. Mol. Life Sci. 59 (6) (2002) 941–949.
[13] J. Rudolph, Cdc25 phosphatases: structure, specificity, and mechanism, Biochemistry 46 (12) (2007) 3595–3604.
[14] R.H. van Huijsduijnen, A. Bombrun, D. Swinnen, Selecting protein tyrosine phosphatases as drug targets, Drug Discovery Today 7 (19) (2002) 1013–1019.
[15] P. Chiarugi, et al., LMW-PTP is a positive regulator of tumor onset and growth, Oncogene 23 (22) (2004) 3905–3914.
[16] H. Park, et al., Structure-based virtual screening approach to identify novel classes of PTP1B inhibitors, Eur. J. Med. Chem. 44 (8) (2009) 3280–3284.
[17] D. Vidal, et al., Structure-based discovery of new small molecule inhibitors of low molecular weight protein tyrosine phosphatase, Eur. J. Med. Chem. 42 (8) (2007) 1102–1108.
[18] H. Park, et al., Structure-based virtual screening approach to identify novel classes of Cdc25B phosphatase inhibitors, Bioorg. Med. Chem. Lett. 19 (15) (2009) 4372–4375.
[19] P.S. Rao, et al., Molecular docking and virtual screening for novel protein tyrosine phosphatase 1B (PTP1B) inhibitors, Bioinformation 8 (17) (2012) 834–837.
[20] R.A. Reynolds, et al., Crystal structure of the catalytic subunit of Cdc25B required for G2/M phase transition of the cell cycle, J. Mol. Biol. 293 (3) (1999) 559–568.
[21] A.P.R. Zabell, et al., Crystal structure of the human B-form low molecular weight phosphotyrosyl phosphatase at 1.6-A resolution, J. Biol. Chem. 281 (10) (2006) 6520–6527.
[22] RCSB Protein Data Bank. http://www.pdb.org/
[23] The PyMOL Molecular Graphics System, Version 1.2r3pre, Schrödinger, LLC.
[24] K.R. Martin, et al., Integrating virtual and biochemical screening for protein tyrosine phosphatase inhibitor discovery, Methods 65 (2) (2014) 219–228.
[25] MOE manual, version 2009.10, Molecular Operating Environment (MOE), Chemical Computing Group, http://www.chemcomp.com/, Montreal, Canada, 2009.
[26] P. Labute, Probabilistic Receptor Potentials, Journal of the Chemical Computing Group, 2001, http://www.chemcomp.com/journal/cstat.htm
[27] Marvin was used for drawing, displaying and characterizing chemical structures, substructures and reactions, Marvin 6.1.3, 2013, ChemAxon, http://www.chemaxon.com/
[28] Timtec Ltd. http://www.timtec.net/
[29] MACCS Keys, MDL Information Systems Inc., 14600 Catalina Street, San Leandro, CA 94577.
[30] T.A. Halgren, MMFF VI. MMFF94s option for energy minimization studies, J. Comput. Chem. 20 (7) (1999) 720–729.
[31] T.A. Halgren, Merck molecular force field. V. Extension of MMFF94 using experimental data, additional computational data, and empirical rules, J. Comput. Chem. 17 (5–6) (1996) 616–641.
[32] T.A. Halgren, Merck molecular force field. I. Basis, form, scope, parameterization, and performance of MMFF94, J. Comput. Chem. 17 (5–6) (1996) 490–519.
[33] T.A. Halgren, Merck molecular force field. III. Molecular geometries and vibrational frequencies for MMFF94, J. Comput. Chem. 17 (5–6) (1996) 553–586.
[34] T.A. Halgren, Merck molecular force field. II. MMFF94 van der Waals and electrostatic parameters for intermolecular interactions, J. Comput. Chem. 17 (5–6) (1996) 520–552.
[35] T.A. Halgren, R.B. Nachbar, Merck molecular force field. IV. Conformational energies and geometries for MMFF94, J. Comput. Chem. 17 (5–6) (1996) 587–615.
[36] T.A. Halgren, Merck molecular force field VII. Characterization of MMFF94, MMFF94s, and other widely available force fields for conformational energies and for intermolecular-interaction energies and geometries, J. Comput. Chem. 20 (7) (1999) 730–748.
[37] L.F. Iversen, et al., Structure-based design of a low molecular weight, nonphosphorus, nonpeptide, and highly selective inhibitor of protein-tyrosine phosphatase 1B, J. Biol. Chem. 275 (14) (2000) 10300–10307.
[38] J.E. Bleasdale, et al., Small molecule peptidomimetics containing a novel phosphotyrosine bioisostere inhibit protein tyrosine phosphatase 1B and augment insulin Action, Biochemistry 40 (19) (2001) 5642–5654.
[39] Application_Name, Scientific Vector Language (SVL) source code provided by Chemical Computing Group Inc., 1010 Sherbooke St. West, Suite #910, Montreal, QC, Canada, H3A 2R7. 2010.
[40] K.M. Branson, B.J. Smith, The role of virtual screening in computer aided structure-based drug design, Aust. J. Chem. 57 (11) (2004) 1029–1037.
[41] A.P. Combs, Recent advances in the discovery of competitive protein tyrosine phosphatase 1B inhibitors for the treatment of diabetes, obesity, and cancer, J. Med. Chem. 53 (6) (2009) 2333–2344.
[42] H.S. Andersen, et al., 2-(Oxalylamino)-benzoic acid is a general, competitive inhibitor of protein-tyrosine phosphatases, J. Biol. Chem. 275 (10) (2000) 7101–7108.
[43] A. Salmeen, et al., Molecular basis for the dephosphorylation of the activation segment of the insulin receptor by protein tyrosine phosphatase 1B, Mol. Cell 6 (6) (2000) 1401–1412.
[44] Z. Jia, et al., Structure of protein tyrosine phosphatase 1B in complex with inhibitors bearing two phosphotyrosine mimetics, J. Med. Chem. 44 (26) (2001) 4584–4594.
[45] L.F. Iversen, et al., Steric hindrance as a basis for structure-based design of selective inhibitors of protein-tyrosine phosphatases, Biochemistry 40 (49) (2001) 14812–14820.
[46] G. Scapin, et al., The structural basis for the selectivity of benzotriazole inhibitors of PTP1B, Biochemistry 42 (39) (2003) 11451–11459.
[47] Z.Y. Zhang, Chemical and mechanistic approaches to the study of protein tyrosine phosphatases, Acc. Chem. Res. 36 (6) (2003) 385–392.
[48] C.A. Lipinski, et al., Experimental and computational approaches to estimate solubility and permeability in drug discovery and development settings, Adv. Drug Del. Rev. 23 (1–3) (1997) 3–25.
[49] D.F. Veber, et al., Molecular properties that influence the oral bioavailability of drug candidates, J. Med. Chem. 45 (12) (2002) 2615–2623.
[50] Molecular Operating Environment (MOE), Chemical Computing Group, http://www.chemcomp.com/, Montreal, Canada, 2009.
[51] S. Wu, et al., In silico screening for PTPN22 inhibitors: active hits from an inactive phosphatase conformation, ChemMedChem 4 (3) (2009) 440–444.
[52] M. Kontoyianni, G.S. Sokol, L.M. McClellan, Evaluation of library ranking efficacy in virtual screening, J. Comput. Chem. 26 (1) (2005) 11–22.
[53] W. Deng, C.L.M.J. Verlinde, Evaluation of different virtual screening programs for docking in a charged binding pocket, J. Chem. Information Model. 48 (10) (2008) 2010–2020.
[54] M.D. Cummings, et al., Comparison of automated docking programs as virtual screening tools, J. Med. Chem. 48 (4) (2005) 962–976.
[55] H. Zhao, et al., Isoxazole carboxylic acids as protein tyrosine phosphatase 1B (PTP1B) inhibitors, Bioorg. Med. Chem. Lett. 14 (22) (2004) 5543–5546.
[56] P.J. Ala, et al., Structural basis for inhibition of protein-tyrosine phosphatase 1B by isothiazolidinone heterocyclic phosphonate mimetics, J. Biol. Chem. 281 (43) (2006) 32784–32795.
[57] Z. Jia, et al., Structural basis for phosphotyrosine peptide recognition by protein tyrosine phosphatase 1B, Science 268 (5218) (1995) 1754–1758.
[58] M.O. Taha, M.A. AlDamen, Effects of variable docking conditions and scoring functions on the qualities of protein aligned CoMFA models constructed from diverse h-PTP 1B inhibitors, J. Med. Chem. 48 (2005) 8016–8034.
[59] C.R. Corbeil, P. Englebienne, N. Moitessier, Docking ligands into flexible and solvated macromolecules. 1. development and validation of FITTED 1.0, J. Chem. Information Model. 47 (2) (2007) 435–449.
[60] K.P. Ravindranathan, et al., Discovery of novel fibroblast growth factor receptor 1 kinase inhibitors by structure-based virtual screening, J. Med. Chem. 53 (4) (2010) 1662–1672.
[61] S.M. Brunskole, et al., Novel inhibitors of trihydroxynaphthalene reductase with antifungal activity identified by ligand-based and structure-based virtual screening, J. Chem. Information Model. 51 (7) (2011) 1716–1724.
[62] M.N. Drwal, R. Griffith, Combination of ligand- and structure-based methods in virtual screening, Drug Discovery Today: Technol. 10 (3) (2013) e395–e401.
[63] S.R. Klopfenstein, et al., 1,2,3,4-Tetrahydroisoquinolinyl sulfamic acids as phosphatase PTP1B inhibitors, Bioorg. Med. Chem. Lett. 16 (6) (2006) 1574–1578.